Turkish Journal of Electrical Engineering & Computer Sciences

http://journals.tubitak.gov.tr/elektrik/

Research Article

Turk J Elec Eng & Comp Sci
(2016) 24: 669 – 682

doi:10.3906/elk-1309-47

Commutation angles adjustment in SRM drives to reduce torque ripple below the motor base speed

Ali SHAHABI*, Amir RASHIDI, Milad AFSHOON, Seyyed Mortaza SAGHAIAN NEJAD
Department of Electrical and Computer Engineering, Isfahan University of Technology, Isfahan, Iran

Received: 09.09.2013 • **Accepted/Published Online:** 10.01.2014 • **Final Version:** 05.02.2016

Abstract: This paper investigates the problem of high torque ripple in switched reluctance motor (SRM) drives. A method is proposed for below the base speed operation of SRM that determines both the turn-off and the turn-on angles for reducing motor torque ripple. Determination of the turn-off angle is an offline process performed through solving a multiobjective optimization function consisting of two criteria: torque ripple and copper loss. Turn-on angle adjustment, however, is an online process based on the intersection approach of consecutive phase currents, particularly proposed in this paper. Simulation and experimental results are presented to validate the reduction in torque ripple gained from the proposed angles control scheme.

Key words: Commutation angles, switched reluctance motor, torque ripple reduction

1. Introduction

Inherent simple structure, robustness, fault tolerance capability, high torque to inertia ratio, and possible operation at high speeds and high temperatures are properties that make the switched reluctance motor (SRM) a strong candidate for various general-purpose adjustable-speed applications. Despite these advantages, one of its drawbacks compared to other conventional machines is the higher torque ripple, which causes vibration and acoustic noise [1].

There are two general approaches to reduce torque ripple. While one approach improves the electromagnetic design of the SRM to reduce torque ripple [2], the other applies electronic control techniques such as instantaneous torque control [3], emotional controllers [4], or passivity-based adaptive sliding mode controllers [5]. Proper adjustment of firing angles is classified under electronic control techniques.

A number of studies have been conducted in the firing angles control field. Relations have been developed in [6] for determination of the turn-off angle to maximize average torque per current. Sozer et al. [7] proposed an automatic turn-on angle control in order to increase the torque to current ratio. In [8], they extended the method by including the turn-off angle as well as the turn-on angle and the reference current. The method was able to affect the torque ripple of the SRM. A hybrid controller has been proposed in which the balanced commutation algorithm is applied in the torque sharing function with the control of central commutation angle θ_c [9]. Fuzzy logic control to vary the value of the turn-off angle based upon the value of current and speed proved to be effective in torque ripple reduction [10]. Mademlis et al. [11] proposed a method to optimize torque ripple and efficiency of the SRM with online adjustment of the turn-on and turn-off angles. A method based on

*Correspondence: a.shahabi@ec.iut.ac.ir

control of flux linkage to determine the optimal commutation angles has been proposed in [12] to improve the performance of the SRM. In [13], low torque ripple and smooth transition between the control operations are achieved by the proposed firing angle control scheme. Xue et al. [14] presented a multiobjective optimization function to improve the performance of SRM drives, including torque ripple, in electric vehicles.

This paper aims to investigate the adjustment of the turn-on and turn-off angles to reduce the torque ripple of the SRM, with emphasis on simplicity and ease of implementation. Through the proposed scheme, the turn-off angle is defined by means of a multiobjective optimization function composed of two criteria: torque ripple factor and copper loss. Minimizing the multiobjective optimization function gives the turn-off angle that realizes a correct balance between torque ripple reduction and copper loss reduction. The turn-on angle is also adjusted by means of a proposed method involving the intersection approach of consecutive phase currents. Using the proposed angles control scheme, torque ripple of the SRM will be reduced. Simulation and experimental results are presented to verify the proposed angles control scheme.

2. Modeling of the SRM

The instantaneous voltage for each phase of the SRM is given by

$$V = Ri + \frac{d\lambda}{dt} \tag{1}$$

The flux linkage in the SRM is a nonlinear function of the rotor position and the motor current. Therefore

$$\frac{d\lambda}{dt} = \frac{\partial\lambda}{\partial i}\frac{di}{dt} + \frac{\partial\lambda}{\partial\theta}\frac{d\theta}{dt} = L(i,\theta)\frac{di}{dt} + e \tag{2}$$

where L is the incremental inductance and e is the back-emf. Figure 2a shows one phase of an asymmetric power converter, used in this study, for a 4-phase SRM. The inductance profile and the running waveforms of the SRM are shown in Figure 2b. In this figure, L_a and L_u are inductances at the aligned position (θ_a) and the unaligned position (θ_u), respectively. Furthermore, θ_p refers to the position of the first peak of the phase current and θ_z is where the phase current becomes zero. Thus, (1) can be written as

$$V = Ri + L(i,\theta)\frac{di}{dt} + e \tag{3}$$

The torque produced by a single phase of SRM is given by

$$T_{ph}(i_{ph},\theta) = \frac{\partial W_c}{\partial\theta}|_{i=cte} \tag{4}$$

where W_c is the phase co-energy. The sum of the instantaneous phase torques gives the total instantaneous torque of SRM

$$T_{inst} = \sum_n T_{ph}(i_{ph},\theta) \tag{5}$$

where n is the number of phases. By integrating the total instantaneous torque in (5), the average torque is derived as follows

$$T_{avg} = \frac{1}{T}\int_0^T T_{inst}dt \tag{6}$$

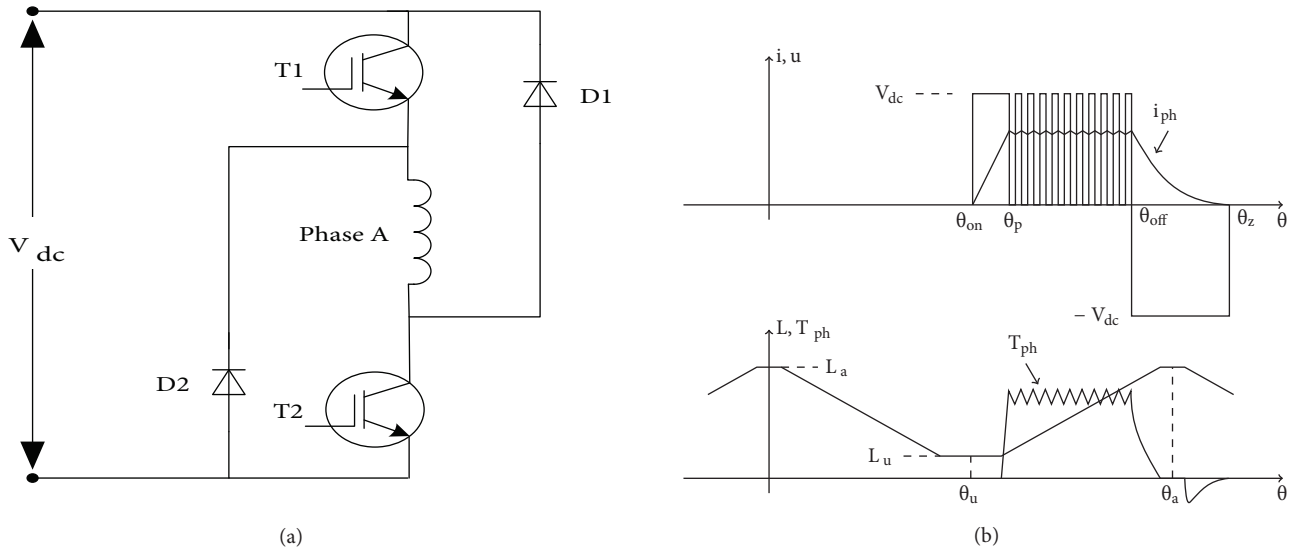

Figure 1. (a) Asymmetric power converter for one phase of a 4-phase SRM, (b) Inductance profile, phase torque, and the running waveforms of a current controlled SRM drive.

The experimental SRM drive has been modeled to support simulation studies; details of the motor specification are given in the Table. Figure 2 shows the SRM characteristic profiles. The rotor position is defined as 0° when the stator pole is fully aligned with the rotor pole.

Torque ripple, K_r, is the difference between the maximum and minimum instantaneous torque, which is expressed as a ratio of the average torque during the steady state operation of the machine

$$K_r = \frac{T_{inst}(max) - T_{inst}(min)}{T_{avg}} \tag{7}$$

For a SRM with n number of phases, the copper loss is proportional to square of the rms current and the winding resistance

$$P_{cu} = nI_{rms}^2 R_{ph} \tag{8}$$

3. Defining the turn-off angle

The aim of this section is to find a proper turn-off angle so that together with proper adjustment of the turn-on angle, low torque ripple performance is achieved at a specified operation point of the SRM. To define a proper turn-off angle, it is desirable to consider the torque ripple criterion and the motor loss criterion simultaneously.

Table. Motor data.

Number of phases	4
Number of stator poles	8
Number of rotor poles	6
Rated power	5.5 hp
DC voltage	280 V
Base speed	1500 rpm
Phase resistance	0.75 Ω
Stroke angle(θ_s)	15°

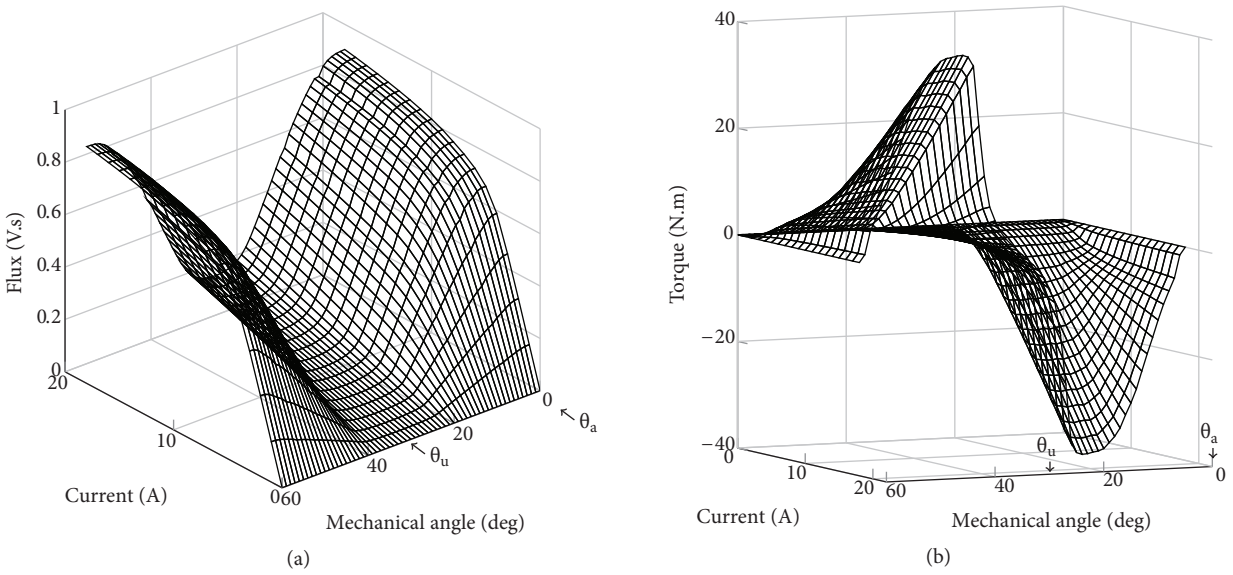

Figure 2. SRM characteristic profiles: (a) Flux linkage, (b) Static torque.

The total loss in motor mainly consists of the copper loss and the iron loss. Iron loss depends on flux density and flux frequency. In this paper, finding the turn-off angle is carried out at a specified load torque and motor speed. Thus, the iron loss variation is small during the turn-off angle optimization [14]. It can be concluded that in this case variation in total loss mainly depends on the variation of copper loss. Therefore, only the copper loss is considered during the optimization process.

In this study, the best motoring operation is regarded as the low torque ripple and the low copper loss. However, realizing each of these goals individually needs different firing angles. In other words, in most cases it is impossible to reduce the torque ripple and the copper loss simultaneously by using the commutation angles. In order to make a desirable compromise between the torque ripple and the copper loss, a multiobjective optimization function that has two groups of weight factors and two groups of base values is applied in this paper. Such a multiobjective optimization function can be written as

$$F_{obj} = W_k \frac{K_r}{K_{rb}} + W_{cu} \frac{P_{cu}}{P_{cub}} \tag{9}$$

$$W_k + W_{cu} = 1 \tag{10}$$

where F_{obj} denotes the multiobjective optimization function, K_r denotes the torque ripple factor, P_{cu} denotes the copper loss, K_{rb} denotes the base value of the torque ripple factor, P_{cub} denotes the base value of the copper loss, W_k denotes the weight factor of the torque ripple factor, and W_{cu} denotes the weight factor of the copper loss. Base values refer to the minimum values of their related criterion at a specific operation point

$$K_{rb}(\theta_{on}, \theta_{off}) \mid_{\omega_r, T_l} = min\{K_r\} \tag{11}$$

$$P_{cub}(\theta_{on}, \theta_{off}) \mid_{\omega_r, T_l} = min\{P_{cu}\} \tag{12}$$

At a specific operation point, K_{rb} and P_{cub} represent the least value of copper loss and torque ripple of motor, obtained through changing firing angles. In fact, at a specific operation point, base values are defined by means

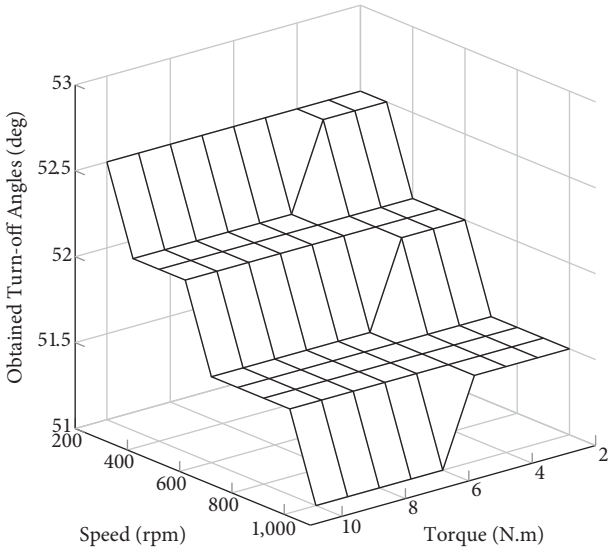

Figure 3. The turn-off angles obtained from minimization of the multiobjective optimization function.

of a search algorithm by which the firing angles are changed step by step and both torque ripple and copper loss are calculated at each step. At the end of the search, the minimum values of copper loss and torque ripple are reported as the base values of the related operation point. Therefore, the 2-D search algorithm is used to find the base values. For the prototype of the four phase SRM drive, the turn-on angle varies from 30° to 40° and the turn-off angle varies from 50° to 59°. The step size for the search is chosen as 0.5°.

The multiobjective optimization function includes two criteria. W_k and W_{cu} imply the expected shares of each criterion, i.e. torque ripple and copper loss, in the optimization function, respectively. Consequently, the optimization function with two objects can be expressed as

$$F_{opt}(\theta_{on}^{opt}, \theta_{off}^{opt}) = min\{W_k \frac{K_r}{K_{rb}} + W_{cu} \frac{P_{cu}}{P_{cub}}\} \tag{13}$$

Solving the above multiobjective optimization function, one can find the proper turn-off angles for various operation points. In this paper, greater importance is attached to the torque ripple than to the copper loss and since the SRM , on which this study is done, has a low winding resistance and, therefore, lower copper loss compared to the other SRM types, it is suggested that the weight factor of the torque ripple should be taken as 0.7 and the weight factor of the copper loss as equal to 0.3. One can apply different weight factors depending on the optimization level required.

Figure 3 shows the turn-off angles obtained from (13) for a prototype 8/6 SRM drive at various load torques and motor speeds. Obviously, the variation in the obtained turn-off angles over a wide range of speeds and torques is relatively small. Therefore, for ease of implementation,one can consider the turn-off angle to be fixed at the average value of the obtained turn-off angles for the entire operation points below the motor base speed . This means no look-up table would be needed for deriving the turn-off angle. Elimination of the look-up table for turn-off angle control results in a much easier experimental implementation. However, to achieve a lower level of torque ripple, a look-up table should be used to store all the data obtained from solving the multiobjective optimization function.

4. Defining the proposed turn-on angle

The mathematical explanation of a SRM is very complicated; therefore, optimization of SRM performance can be analytically approached through motor running waveforms. Simulation and experimental tests indicate that the turn-on angle should be adjusted in a particular way in order to reduce the torque ripple of the SRM in PWM mode operation and below the motor base speed. This paper suggests that in PWM mode and below the motor base speed, the turn-on angle should be adjusted in such a way that the incoming phase current reaches the current reference value at the turn-off point of the outgoing phase. Figure 4a depicts this issue.

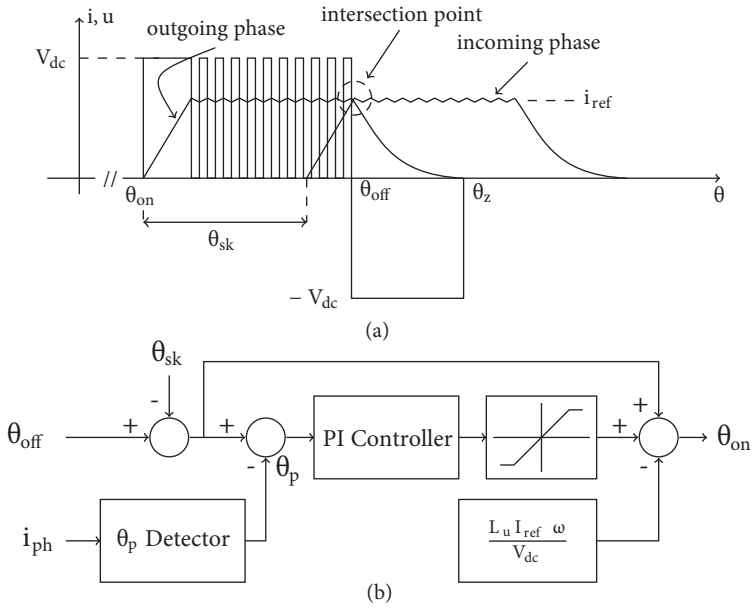

Figure 4. (a) SRM running waveforms considering the proposed method on intersection approach of consecutive phase currents, (b) The proposed turn-on angle control system.

The instantaneous voltage across the terminals of a single winding of SRM can be expressed by (3). The turn-on point of the phases in SRM is considered to be located at the minimum inductance region of the inductance profile due to utilization of the maximum capability of the motor in torque production. In this region, therefore, the incremental inductance, L, is almost equal to the inductance at the unaligned position. By ignoring the phase resistance, (R), and the back-emf expression, ($e = \frac{\partial \lambda}{\partial \theta}\frac{d\theta}{dt}$), and replacing the incremental inductance with the unaligned inductance, (3) can be approximated as

$$V = \frac{\partial \lambda}{\partial i}\frac{di}{dt} = L_u.\frac{di}{dt} \tag{14}$$

where L_u is the inductance at the unaligned position. Multiplying each side of (14) by the differential, $d\theta$, and solving for $d\theta$, give

$$d\theta = \frac{L_u.di}{V}.\frac{d\theta}{dt} \tag{15}$$

and the advanced angle yields

$$\theta_{adv} = \frac{L_u I_{ref}\omega}{V_{dc}} \tag{16}$$

where θ_{adv} is the displacement angle needed to advance the turn-on angle from $\theta_{off} - \theta_{sk}$ angle in order to make the first peak of the incoming phase current at the turn-off point of the outgoing phase current. θ_{sk} is the stroke angle. Consequently, the turn-on angle should be adjusted as

$$\theta_{on} = \theta_{off} - \theta_{sk} - \theta_{adv} = \theta_{off} - \theta_{sk} - \frac{L_u I_{ref} \omega}{V_{dc}} \tag{17}$$

In deriving (17), the back-emf expression was ignored. Basically, calculating the back-emf value is not easy. This may cause some errors in defining the right turn-on angle. Therefore, it is desirable to have a closed loop control that compensates for the absence of the back-emf effect in (17). The closed loop control algorithm continuously monitors the position of the first peak of the phase current (θ_p). The error between θ_p and the turn-off angle of the outgoing phase, $\theta_{off} - \theta_{sk}$, is directed to a PI controller. Based on the error, the PI controller adds a term to (17) and compensates for absence of the back-emf. Adjustment of the PI controller is done through the common adjustment procedures of PI controllers. The turn-on angle is, consequently, advanced or retarded automatically to place θ_p on the θ_{off} angle of the outgoing phase. The control of θ_{on} in PWM mode is summarized in Figure 4b.

5. Implementation of the proposed angles controller system

Figure 5 shows the block diagram of the SRM drive with the proposed angles control system. An adjusted PI controller is used to build up the reference current, i_{ref}, through the speed error $(\omega_{ref} - \omega_r)$. The switch pulses block is used to produce switching pulses by applying a PWM current controller with unipolar strategy.

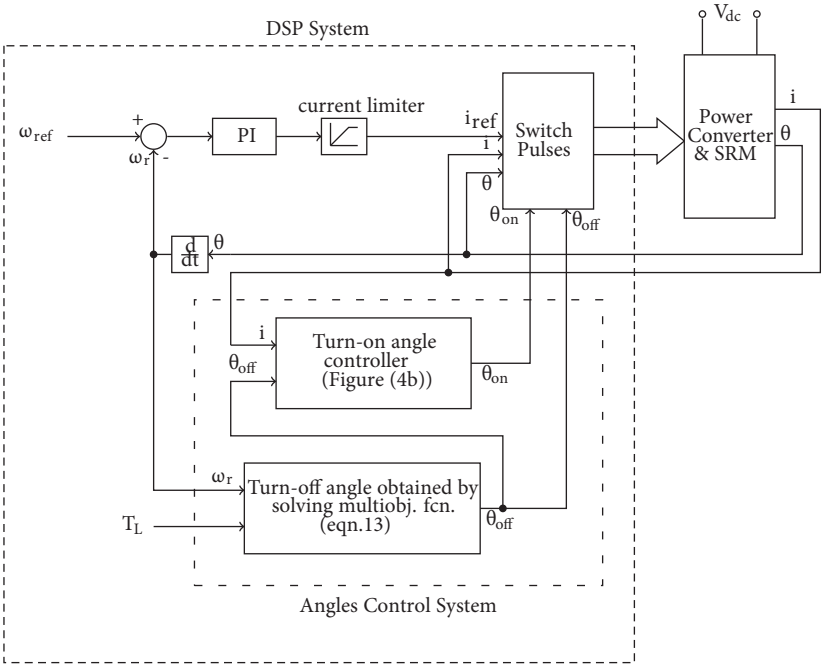

Figure 5. Block diagram of the SRM drive with the proposed angles control system.

At each operating point, as illustrated in Figure 5, the turn-on and turn-off angles are determined by the proposed angles control system. To determine the proper turn-off angle, the multiobjective optimization

function (13) with two criteria, i.e. the torque ripple factor and the copper loss, is defined and solved. Solving the multiobjective optimization function is, in fact, minimizing its value through varying its parameters θ_{on} and θ_{off}. At each operation point, there is a turn-off angle, along with a fine-adjusted turn-on angle, by which the torque ripple is considerably reduced. Solving the multiobjective optimization function determines the proper turn-off angle. Defining the turn-off angle is an offline process. The turn-off angle of each operating point can be stored in a look-up table to be used in the runtime. The turn-on angle is also determined by means of the proposed control algorithm explained in Section 4 and shown in Figure 4b.

6. Simulation and experimental results

The angles control algorithm introduced in this paper has been implemented for simulation. The SRM on which the simulations are based is a four phase, 5.5 hp, 8/6 SRM. The motor parameters are given in the Table. The algorithm has also been experimentally implemented on the same SRM using an eZdsp TMS320F28335 board. The SRM is coupled to a DC generator, which serves as a load torque. The used power converter is an asymmetric one. The instantaneous torque of the motor has been estimated by means of a look-up table with phase currents and rotor position as its inputs.

Figures 6–8 depict the performance of the proposed angles controller shown in Figure 5 together with the performance of the fixed-angle operation and the performance of the method presented in [11]. The proposed angles controller adjusts the turn-off angle based on the values obtained from solving the multiobjective optimization function and then drives the changes in θ_{on} in order to force the first peak of the incoming phase current happening at the turn-off point of the outgoing phase.

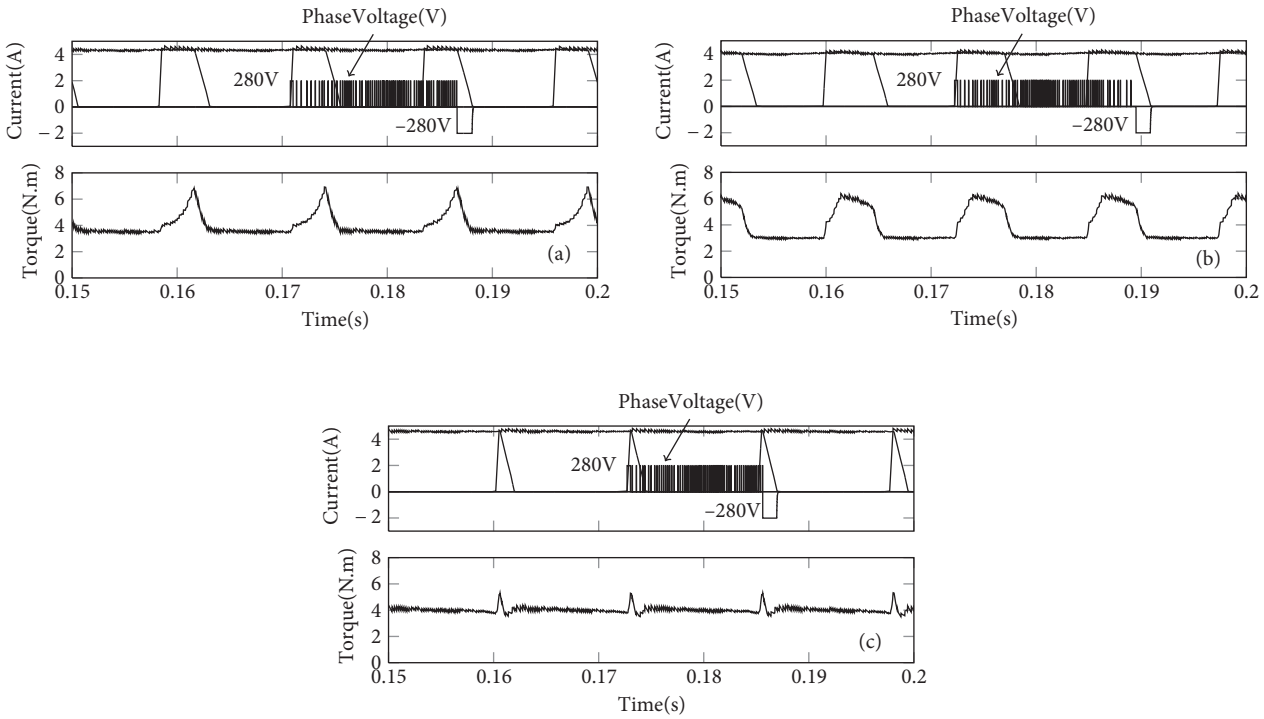

Figure 6. Simulation results at $\omega_r = 200$ rpm and $T_L = 4$ N.m: (a) fixed-angle operation ($\theta_{on} = 35^\circ$, $\theta_{off} = 54^\circ$), (b) operation of method in [11], (c) operation of the proposed angles controller.

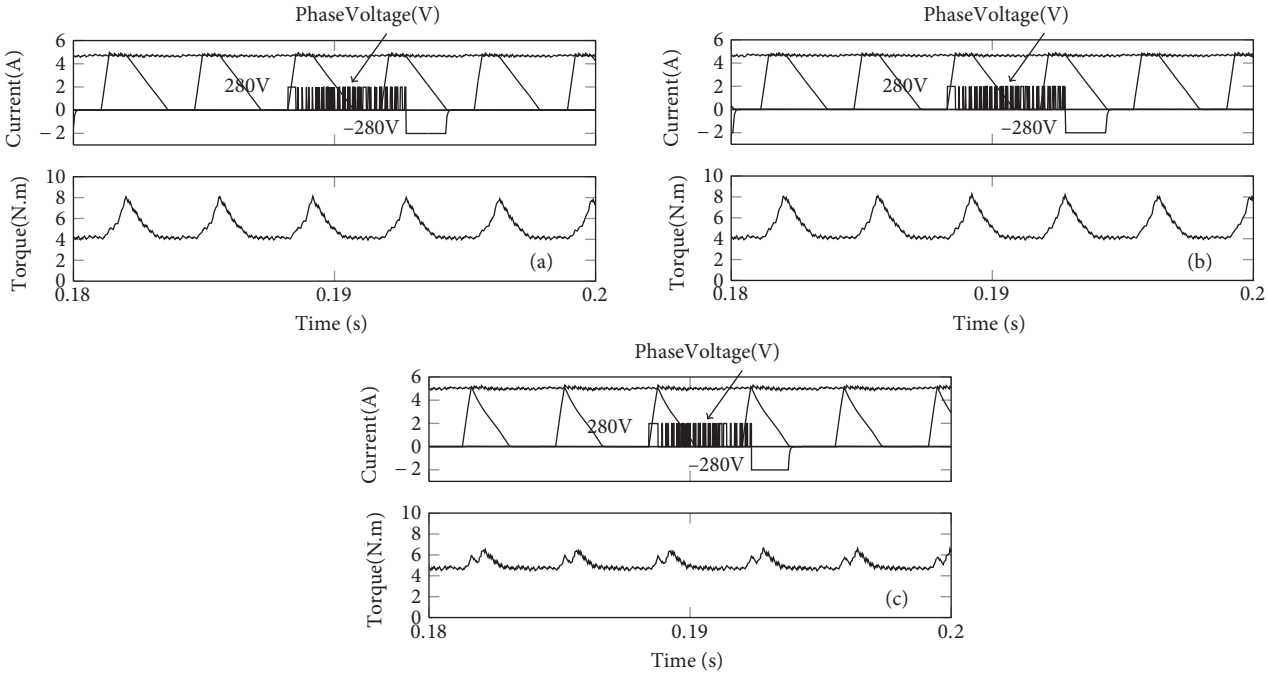

Figure 7. Simulation results at $\omega_r = 700$ rpm and $T_L = 5$ N.m: (a) fixed-angle operation ($\theta_{on} = 35^\circ$, $\theta_{off} = 54^\circ$), (b) operation of method in [11], (c) operation of the proposed angles controller.

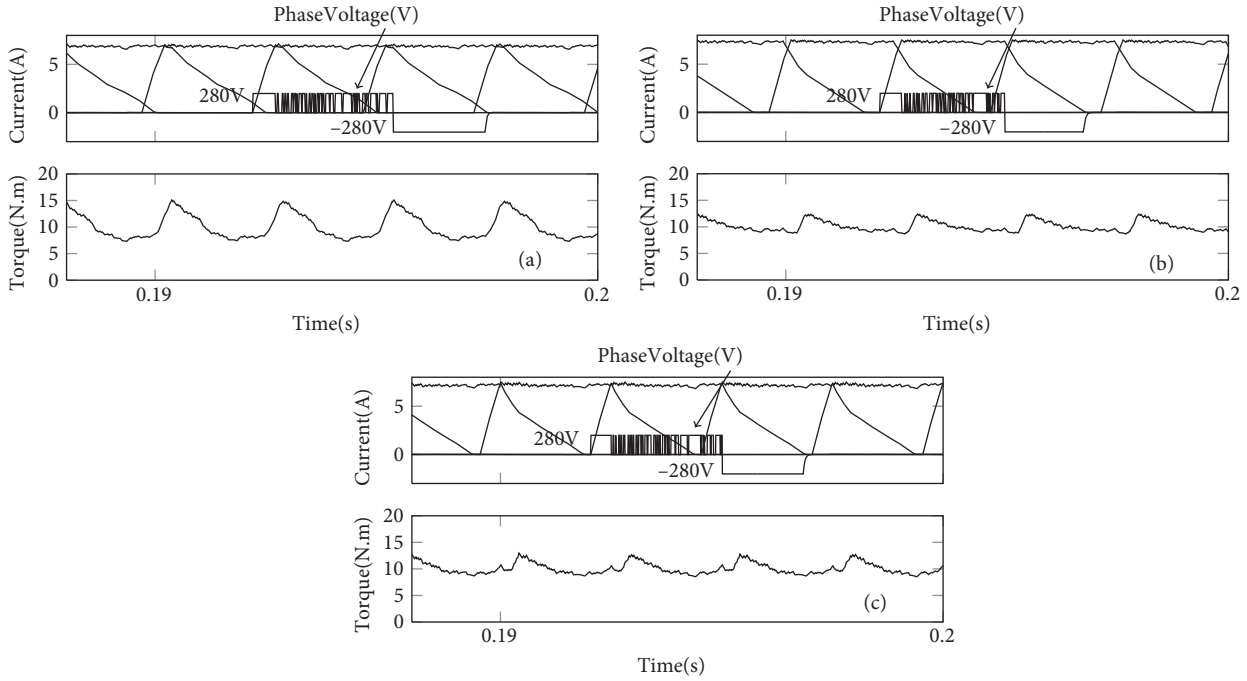

Figure 8. Simulation results at $\omega_r = 1000$ rpm and $T_L = 10$ N.m: (a) fixed-angle operation ($\theta_{on} = 35^\circ$, $\theta_{off} = 54^\circ$), (b) operation of method [11], (c) operation of the proposed angles controller.

The transient responses of the proposed angles controller are shown in Figure 9 for both command speed step-changes and load torque disturbance. The proposed angles controller changes the turn-off angle

immediately due to the change in operation point by using the data stored in the look-up table; however, the turn-on angle is online adjusted by following the explained scheme.

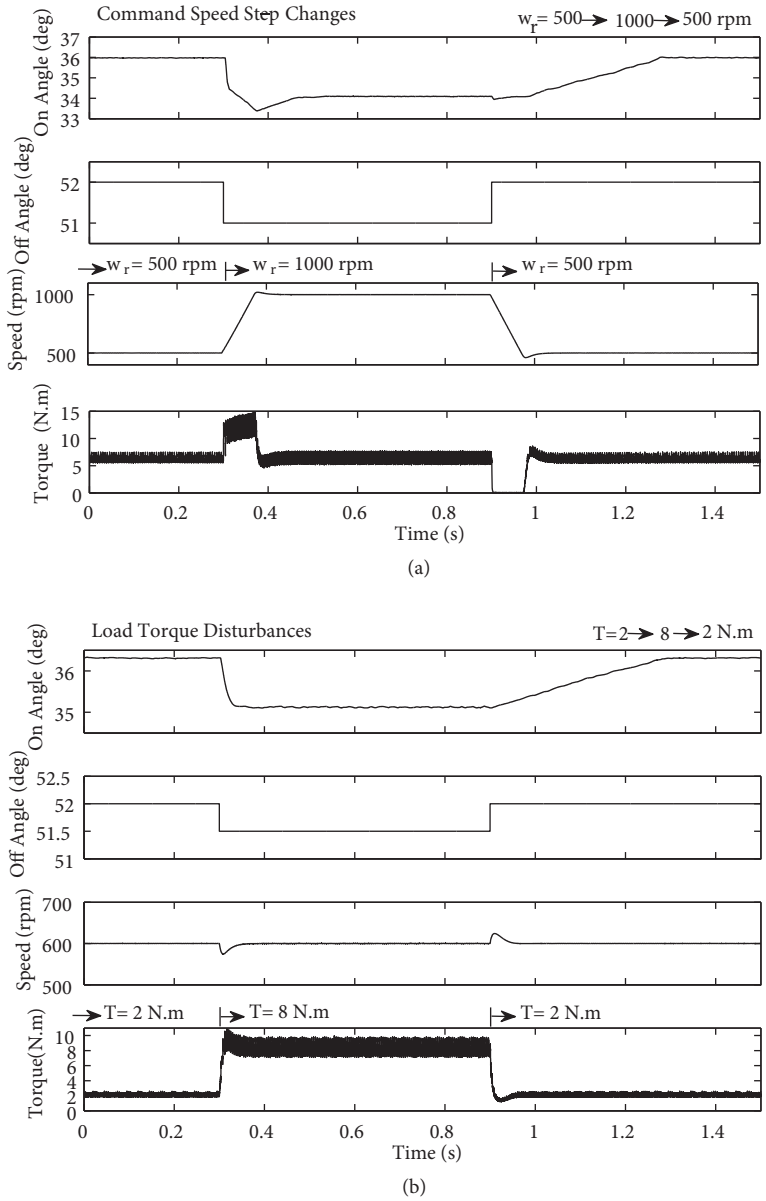

Figure 9. Responses of the proposed angles control system to: (a) command speed step-changes at 6 N.m from 500 rpm to 1000 rpm to 500 rpm and (b) load torque disturbances at 600 rpm from 2 N.m to 8 N.m to 2 N.m.

Figure 10 illustrates variation of the turn-on and turn-off angles, obtained by the proposed scheme, versus load torque for various speed values. Figure 11 compares the torque ripple factor obtained from the proposed angles controller with the ones obtained from operation in minimum torque ripple, the method proposed in [11], and the fixed-angle operation. These comparisons show that the proposed method results in lower torque ripple of the SRM below the motor base speed compared to other methods. In fact, the proposed method shows its advantage below the base speed of motor such that low torque ripple close to the minimum achievable torque

ripple by adjustment of the firing angles is obtained. The torque and copper loss performance of the proposed scheme are illustrated in Figure 12, where the proposed scheme is applied to the test SRM. It can be observed that K_r/K_{rb} changes in range from 1.1 to 1.32 and P_{cu}/P_{cub} is between 1.05 and 1.13.

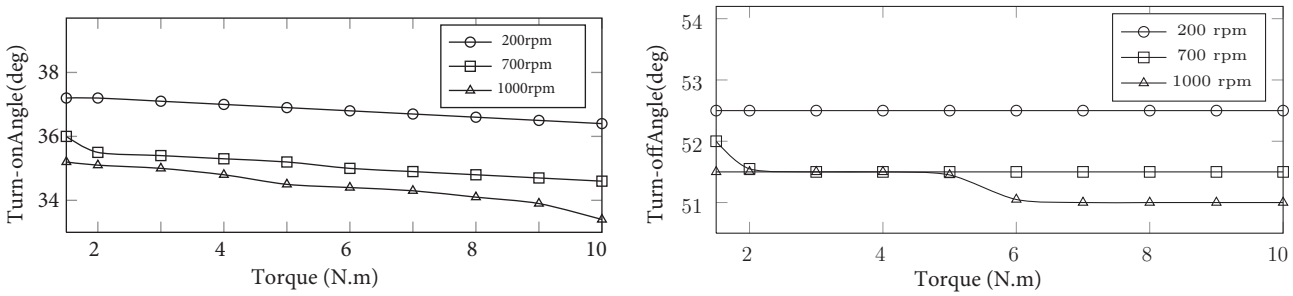

Figure 10. Variation of the obtained turn-on and turn-off angles versus torque for various speeds.

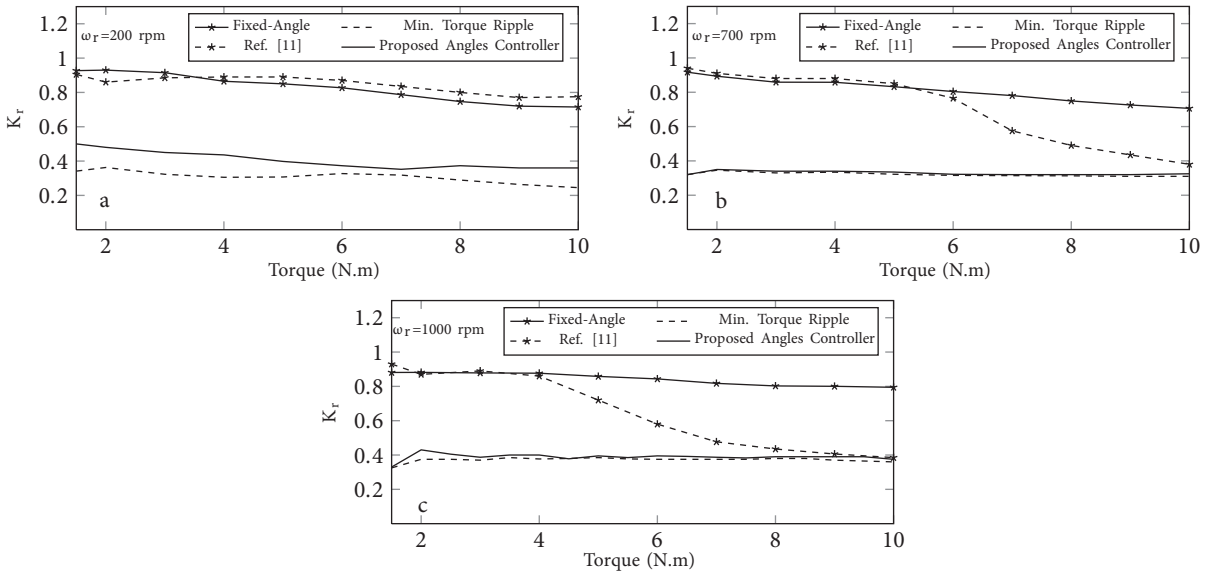

Figure 11. Torque ripple comparison of the proposed scheme with those of operation in fixed-angle ($\theta_{on} = 35^\circ$, $\theta_{off} = 54^\circ$), the method used in [11], and operation in minimum torque ripple: (a) 200 rpm, (b) 700 rpm, (c) 1000 rpm.

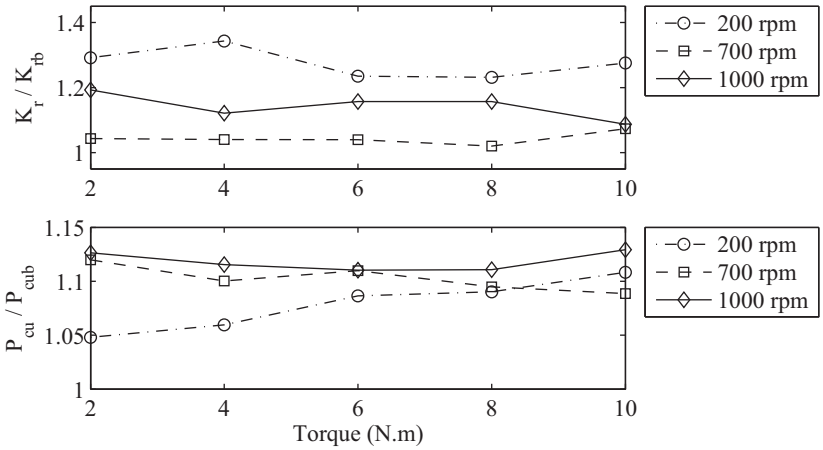

Figure 12. Torque ripple and copper loss performance of the proposed scheme.

Figure 13 shows the experimental setup. Figures 14 and 15 depict the experimental results of the test SRM. The experimental results of the proposed angles controller are depicted together with those of two fixed-angle operation cases. The results from the experimental setup have been prepared for two operation points.

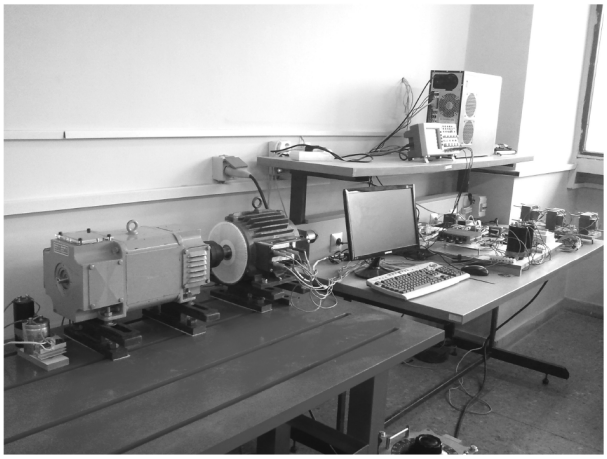

Figure 13. SRM experimental setup.

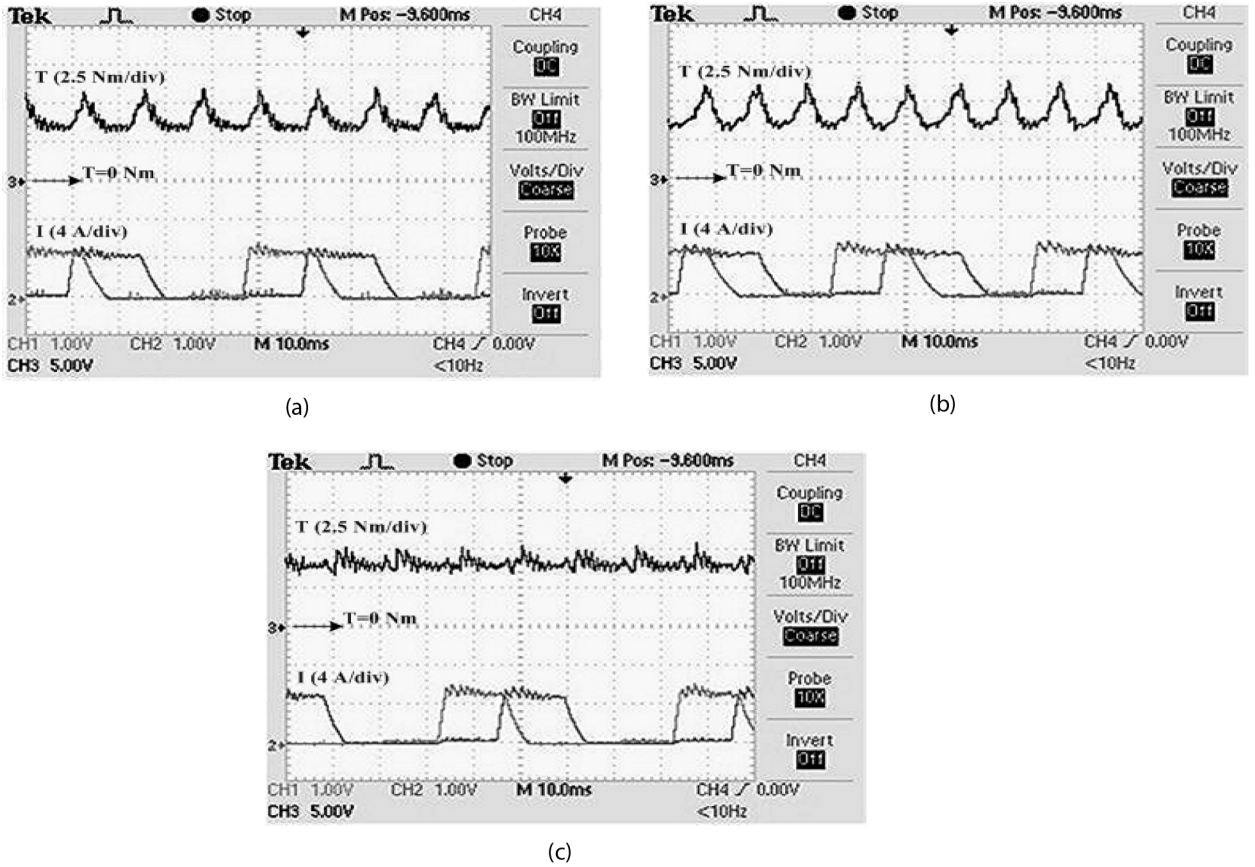

Figure 14. Phase currents and estimated torque at $\omega_r =$ 200 rpm, $T_L =$ 4 N.m: (a) $\theta_{on} = 35^\circ$, $\theta_{off} = 54^\circ$, (b) $\theta_{on} = 32^\circ$, $\theta_{off} = 56^\circ$, (c) operation of the proposed angles controller.

As is obvious, the proposed angles controller manages the firing angles so that the torque ripple of the motor remains low. Comparison of the proposed angles controller performance with the performance of the fixed-angles operation verify the effectiveness of the proposed scheme in torque ripple reduction. Therefore, in addition to the simulation results, the experimental results verify the proper operation of the proposed angles controller and its effectiveness too.

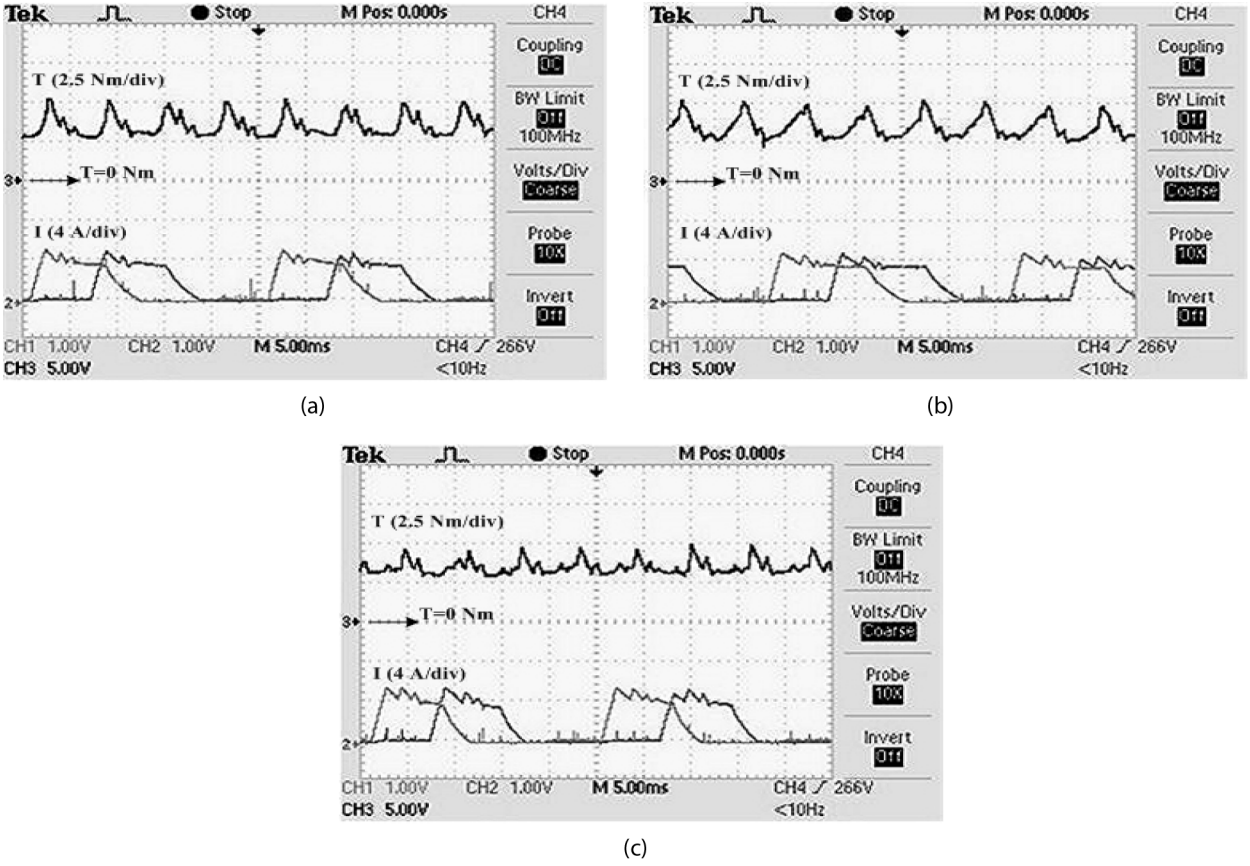

Figure 15. Phase currents and estimated torque at $\omega_r =$ 400 rpm, $T_L =$ 3 N.m: (a) $\theta_{on} = 35^\circ$, $\theta_{off} = 54^\circ$, (b) $\theta_{on} = 32^\circ$, $\theta_{off} = 56^\circ$, (c) operation of the proposed angles controller.

7. Conclusion

In this paper, the problem of torque ripple in current controlled SRM drives has been investigated. The goal involves finding the proper firing angles by which the SRM experiences low torque ripple below the motor base speed. A method to adjust the firing angles has been proposed. Being offline, the turn-off angle is adjusted via solving a multiobjective optimization function consisting of two criteria: the torque ripple factor and the copper loss. The turn-on angle adjustment, however, is online. It is adjusted so that the incoming phase current reaches the current reference value exactly at the turn-off point of the outgoing phase. A simple formula for the proposed turn-on angle has been derived and a control system has been applied to compensate for absence of the back-emf effect in deriving the formula. The proposed turn-on angle control is simple and easy to implement since exact knowledge of the SRM model is not needed. Finally, simulation and experimental results on a prototype SRM drive and comparisons have been presented to validate the operational improvements of the proposed angles control scheme.

References

[1] Krishnan R. Switched Reluctance Motor Drives: Modeling, Simulation, Analysis, Design, and Applications. Boca Raton, FL, USA: CRC Press, 2001.

[2] Sahin C, Amac AE, Karacor M, Emadi A. Reducing torque ripple of switched reluctance machines by relocation of rotor moulding clinches. IET Electr Power App 2012; 6: 753–760.

[3] Wong KF, Cheng KWE, Ho SL. On-line instantaneous torque control of a switched reluctance motor based on co-energy control. IET Electr Power App 2009; 3: 254–264.

[4] Daryabeigi E, Emanian A, Namazi MM, Rashidi A, Saghaian-Nejad SM. Torque ripple reduction of switched reluctance motor (SRM) drives, with emotional controller (BELBIC). In: Twenty-Seventh Annual IEEE Applied Power Electronics Conference and Exposition (APEC); 5–9 Feb 2012; Orlando, FL, USA. New York, NY, USA: IEEE. pp. 1528–1535.

[5] Isfahani MMN, Saghaian-Nejad SM, Rashidi A, Zarchi HA. Passivity-based adaptive sliding Mode speed control of switched reluctance motor drive considering torque ripple reduction. In: IEEE International Electric Machines & Drives Conference (IEMDC); 15–18 May 2011; Niagara Falls, Canada. New York, NY, USA: IEEE. pp. 1480–1485.

[6] Gribble JJ, Kjaer PC, Miller TJE. Optimal commutation in average torque control of switched reluctance motors. In: IEE Proceedings Electric Power Applications; Jan 1999. Stevenage, UK: IET. pp. 2–10.

[7] Sozer Y, Torrey DA, Mese E. Automatic control of excitation parameters for switched-reluctance motor drives. IEEE T Power Electr 2003; 18: 594–603.

[8] Sozer Y, Torrey DA. Optimal turn-off angle control in the face of automatic turn-on angle control for switched-reluctance motors. IET Electr Power App 2007; 1: 395–401.

[9] Husain I. Minimization of torque ripple in SRM drives. IEEE T Ind Electron 2002; 49: 28–39.

[10] Rodrigues M, Costa Branco PJ, Suemitsu W. Fuzzy logic torque ripple reduction by turn-off angle compensation for switched reluctance motors. IEEE T Ind Electron 2001; 48: 711–715.

[11] Mademlis C, Kioskeridis I. Performance optimization in switched reluctance motor drives with online commutation angle control. IEEE T Energy Conver 2003; 18: 448–457.

[12] Kioskeridis I, Mademlis C. Maximum efficiency in single-pulse controlled switched reluctance motor drives. IEEE T Energy Conver 2005; 20: 809–817.

[13] Mademlis C, Kioskeridis I. Four-quadrant smooth torque controlled Switched Reluctance Machine drives. In: IEEE Power Electronics Specialists Conference; 5–19 June 2008; Rhodes, Greece. New York, NY, USA: IEEE. pp. 1216–1222.

[14] Xue XD, Cheng KWE, Lin JK, Zhang Z, Luk KF, Ng TW, Cheung NC. Optimal control method of motoring operation for SRM drives in electric vehicles. IEEE T Veh Technol 2010; 59: 1191–1204.